Regular Article

Accountability of Modern Adiabatic Connection-Based Double-Hybrids Constructed from Cubic and Quadratic Integrand Functions for Dipole Polarizabilities of Water Nanoclusters

M. Alipour*

Department of Chemistry, College of Sciences, Shiraz University, Shiraz, Iran

In this work, we dissect the performance of two modern Perdew-Burke-Ernzerhof (PBE)-based double-hybrid (DH) density functionals to predict the isotropic and anisotropic polarizabilities of water nanoclusters $(H_2O)_n$ [n = 2-6]. The considered models include the cubic integrand (CI) and quadratic integrand (QI) functions as well as the spin-opposite-scaled (SOS) scheme for perturbative correlation term. It is shown that all the tested CIDHs and QIDHs underestimate the isotropic polarizabilities, while in the case of anisotropic polarizabilities there is also overestimation of data for a few of nanoclusters when employing the PBE-QIDH-OS model. Putting all the results together, the recommended DH functionals for predicting the dipole polarizabilities of water nanoclusters turned out to be PBE-CIDH, PBE-CIDH-OS, PBE-QIDH, and PBE0-DH with deviations smaller than those provided from Møller-Plesset perturbation calculations.

INTRODUCTION

Since the publication of the first double-hybrid (DH) density functional, B2-PLYP [1], the DH density functional theory (DH-DFT) approximations have received remarkable attention in the literature [2-4]. The story behind DHs is the same as in the single-hybrid (SH) density functionals. In fact, while in SHs only a contribution of the DFT exchange is replaced by Hartree-Fock (HF) exchange, the DH functionals additionally substitute part of the DFT correlation with a nonlocal correlation contribution from second-order Møller-Plesset (MP2) perturbation theory. The energy expression of DH exchange-correlation (XC) functionals can thus be written as follows,

$$E_{xc}^{DH} = w_x^{HF} E_x^{HF} + (1 - w_x^{HF}) E_x^{DFT} + \left(1 - w_c^{MP2}\right) E_c^{DFT} + w_c^{MP2} E_c^{MP2} \quad (1)$$

Here, E_x^{HF} and E_c^{MP2} are the HF exchange energy and MP2 correlation energy with the fractions of w_x^{HF} and w_c^{MP2},

*Corresponding author. E-mail: malipour@shirazu.ac.ir

respectively. The two other terms, E_x^{DFT} and E_c^{DFT}, denote the semilocal exchange and correlation energies, respectively. The parameters w_x^{HF} and w_c^{MP2} in Eq. (1) can be determined empirically (*parameterized* or *empirical* models) or theoretically (*parameter-free* or *nonempirical* models) [5-30].

In recent years, several reformulations of DH density functionals have also been proposed [11,12]. As one of them, which recently served as a motivation for developing the parameter-free DHs, the linearly scaled one-parameter double-hybrid (LS1DH) approximation with only one parameter (λ) can be noted [12],

$$E_{xc}^{LS1DH, \lambda} = \lambda E_x^{HF} + (1 - \lambda) E_x^{DFT}[\rho] + (1 - \lambda^3) E_c^{DFT}[\rho] + \lambda^3 E_c^{MP2} \quad (2)$$

From a different perspective [19], we are lately witness the blooming of DH functionals constructed from another approach, namely the adiabatic-connection (AC) formalism [31]. The two modern AC-based DH models in concern are quadratic integrand double-hybrid (QIDH) [24] and cubic integrand double-hybrid (CIDH) [25] functionals. In the

QIDH model, the energy expression has been constructed by employing a QI function as approximate XC integrand using the equation below [24],

$$E_{xc,\lambda_x}^{\text{QIDH}}[\rho] = \frac{\lambda_x + 2}{3} E_x^{\text{HF}} + \frac{1-\lambda_x}{3} E_x^{\text{DFT}}[\rho] + \frac{2}{3} E_c^{\text{DFT}}[\rho] + \frac{1}{3} E_c^{\text{MP2}}[\rho] \quad (3)$$

On the other hand, the CIDH model has recently been proposed by the present author [25] who uses the following energy expression based on a CI function as approximate XC integrand,

$$E_{xc,\lambda_x}^{\text{CIDH}}[\rho] = \frac{\lambda_x + 1}{2} E_x^{\text{HF}} + \frac{1-\lambda_x}{2} E_x^{\text{DFT}}[\rho] + \frac{5}{6} E_c^{\text{DFT}}[\rho] + \frac{1}{6} E_c^{\text{MP2}}[\rho] \quad (4)$$

In QIDH and CIDH protocols the value of λ_x is determined using the LS1DH approximation, Eq. (2), as $\lambda_x = 3(3)^{-1/3} - 2$ and $\lambda_x = 2(6)^{-1/3} - 1$, respectively.

The DH density functionals have also been designed within the framework of spin-component-scaled (SCS) scheme in which MP2 correlation energy can systematically be improved by separate scaling of the opposite-spin (OS) and same-spin (SS) components [32], see for instance Refs. [8,14,18]. Moreover, another version of DHs based on OS approach [33] may also be considered where only contributions of electron pairs with opposite spin are taken into account for the perturbative correlation term [9,10].

Recently, the performance of various parameterized and parameter-free DHs for predicting the dipole polarizabilities of hydrogen-bonded systems has been assessed [23]. Working in this line, it has been shown that the DH density functionals, and especially the parameter-free ones, have superior performance with respect to the approximations from previous rungs of Jacob's ladder [34]. Despite earlier studies on the applicability of DHs for response properties, there are still some drawbacks in this arena and the quest for a better functional continues. In this respect, the performance of the two most recently proposed DH models, CIDH and QIDH, and their OS versions have not been benchmarked yet on dipole polarizabilities of water nanoclusters as representative examples of hydrogen-bended systems. Hereby, we have undertaken this issue in the current contribution.

DETAILS OF CALCULATIONS

To construct the working expressions for CIDHs and QIDHs as well as the OS counterparts, the exchange and correlation terms in Eqs. (3) and (4) should be specified. We have utilized the widely used Perdew-Burke-Ernzerhof (PBE) approximation [35] for this purpose and consequently the four models, PBE-CIDH, PBE-QIDH, PBE-CIDH-OS and PBE-QIDH-OS, are derived. It has earlier been pointed out that the dipole polarizabilities are well predicted by functionals including the PBE exchange and correlation approximations [23]. In addition, another advantage of choosing PBE is its nonempirical background, so that in this manner we obtain the functionals free of any fitted parameter. Following previous suggestions [36], the aug-cc-pVDZ basis set was used in our calculations. However, for more details on the effects of basis sets on response properties of hydrogen-bonded systems see, for instance, the detailed works of Maroulis on linear and nonlinear polarizabilities of monomer and dimer of water [37,38]. As a reference to evaluate the performance of functionals, the CCSD/aug-cc-pVDZ model chemistry has been employed. All the runs of the present calculations have been implemented in Gaussian09 suite of codes [39]. The usual statistical metrics such as mean signed deviation (MSD), mean absolute deviation (MAD), and maximum absolute deviation (MaxAD) were used for statistical analyses of data. Atomic units (a.u.) are used throughout.

RESULTS AND DISCUSSION

Shown in Fig. 1 are the geometrical structures of water nanoclusters $(H_2O)_n$ [n = 2-6] ranging in size from the dimer to four different isomers of the hexamer optimized at the CCSD/aug-cc-pVDZ level of theory [40]. To explore the effects of the shape of clusters on the computed dipole polarizabilities and consequently the accountability of the tested AC-based DHs for predicting the corresponding data, we have considered more than one structure for the water hexamer. The values of signed deviations of the computed isotropic ($\overline{\alpha}$) and anisotropic ($\Delta\alpha$) dipole polarizabilities of these nanoclusters using the CIDHs and QIDHs are reported in Table 1. Moreover, the corresponding graphical representations are plotted in Figs. 2a and 2b, respectively.
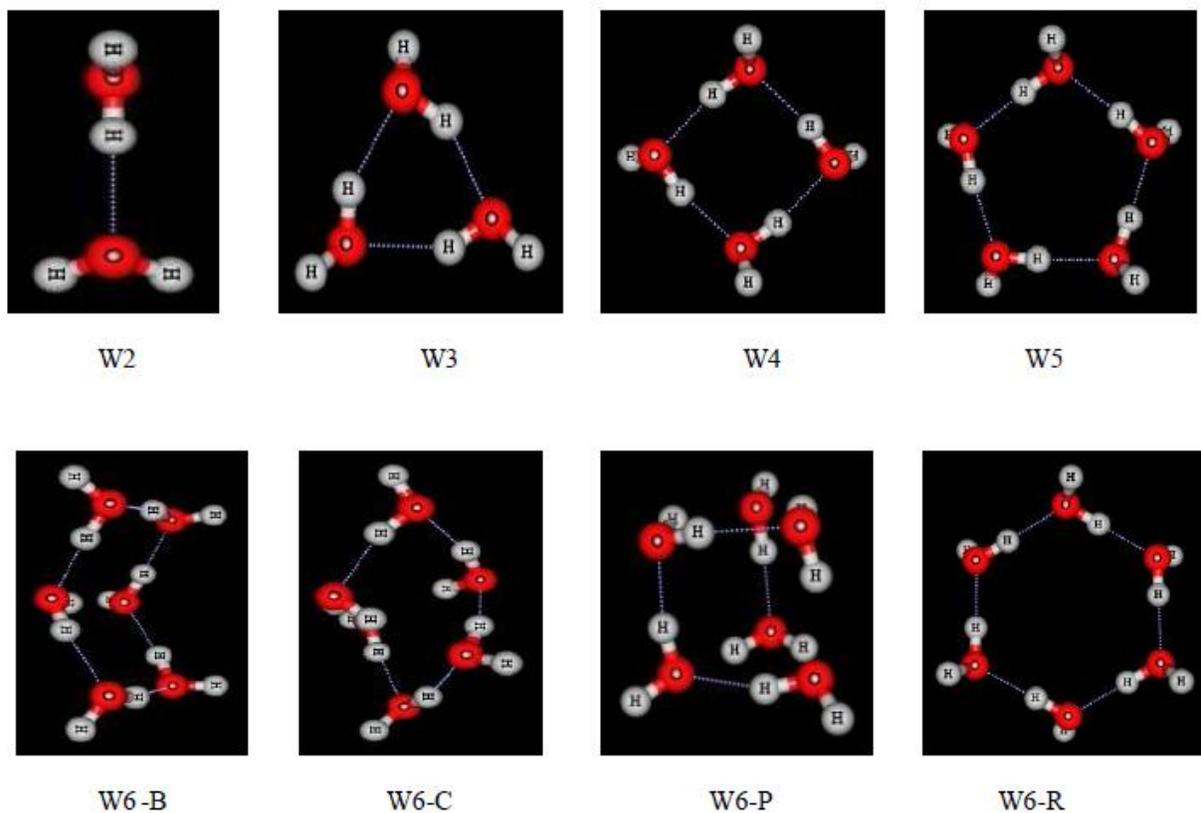
Fig. 1. CCSD/aug-cc-pVDZ optimized structures of water nanoclusters $(H_2O)_n$ [n = 2-6] under study. Color conventions: red for oxygen and light gray for hydrogen. The used tags are as follows; W2: $(H_2O)_2$, W3: $(H_2O)_3$, W4: $(H_2O)_4$, W5: $(H_2O)_5$, W6-B: $(H_2O)_6$-Book, W6-C: $(H_2O)_6$-Cage, W6-P: $(H_2O)_6$-Prism, and W6-R: $(H_2O)_6$-Ring.

Based on the present results, PBE-CIDH, PBE-QIDH, and their OS versions have similar patterns on signed deviations of isotropic polarizabilities (Fig. 2a). Obviously, the deviations have a linear decreasing pattern with the cluster size up to water hexamer. For different hexamers, however, the variations of signed deviations in different functionals are very smooth. In the case of anisotropic polarizabilities, Fig. 2b, the trend of deviations is more pronounced, indicating that the values of $\Delta\alpha$ are more affected by the hydrogen bonding patterns. On the other hand, we find from the figures that all the tested models underestimate the values of isotropic polarizabilities while the values of deviations do not change systematically in the case of anisotropic polarizabilities. In the latter case, although the

overestimation of data is more apparent, the anisotropic polarizabilities are also found to be underestimated for a few nanoclusters when employing the PBE-QIDH-OS functional.

The issue of signed deviations aside, general evaluation of the performance of functionals has been performed using MADs and MaxADs. The corresponding statistical descriptors of our analyses are gathered in Table 2. Moreover, to make the key trends more visible, absolute deviations in the computed values of $\overline{\alpha}$ and $\Delta\alpha$ using the benchmarked DHs are exhibited in Figs. 3a and 3b, respectively. We first evaluate the results of isotropic polarizabilities for the water nanoclusters under consideration. Our numerical data show that the most

Table 1. Signed Deviations (Calc.-Ref.) on the Computed Values of Isotropic and Anisotropic Polarizabilities (a.u.) Using the CIDH and QIDH Models for the Water Nanoclusters under Study; Also Listed are the CCSD Results as Reference Data

Method	W2	W3	W4	W5	W6-B	W6-C	W6-P	W6-R
	$\overline{\alpha}$ [a]							
PBE-CIDH	-0.12	-0.10	-0.17	-0.22	-0.23	-0.18	-0.16	-0.27
PBE-CIDH-OS	-0.33	-0.44	-0.64	-0.81	-0.95	-0.89	-0.88	-0.98
PBE-QIDH	-0.19	-0.23	-0.35	-0.45	-0.51	-0.45	-0.44	-0.54
PBE-QIDH-OS	-0.54	-0.79	-1.11	-1.40	-1.67	-1.61	-1.60	-1.70
CCSD	18.59	28.12	37.92	47.66	57.00	56.39	56.04	57.36
	$\Delta\alpha$ [b]							
PBE-CIDH	0.11	0.22	0.24	0.30	0.29	0.19	0.09	0.34
PBE-CIDH-OS	0.05	0.15	0.07	0.07	0.08	0.08	0.09	0.04
PBE-QIDH	0.05	0.12	0.11	0.12	0.12	0.07	0.05	0.12
PBE-QIDH-OS	-0.04	0.02	-0.17	-0.24	-0.20	-0.09	0.05	-0.36
CCSD	3.47	5.22	7.10	9.15	8.80	7.70	5.21	10.55

[a] $\overline{\alpha} = \frac{1}{3}\left(\alpha_{xx} + \alpha_{yy} + \alpha_{zz}\right)$. [b] $\Delta\alpha = \left(\frac{1}{2}\right)^{1/2}\left[\left(\alpha_{xx} - \alpha_{yy}\right)^2 + \left(\alpha_{xx} - \alpha_{zz}\right)^2 + \left(\alpha_{zz} - \alpha_{yy}\right)^2 + 6\left(\alpha_{xy}^2 + \alpha_{xz}^2 + \alpha_{zy}^2\right)\right]^{1/2}$.

Table 2. Performance of CIDHs and QIDHs for Computing the Isotropic and Anisotropic Polarizabilities (a.u.) of Water Nanoclusters under Study

	$\overline{\alpha}$		$\Delta\alpha$	
Method	MAD	MaxAD	MAD	MaxAD
PBE-CIDH	0.18	0.27	0.22	0.34
PBE-CIDH-OS	0.74	0.98	0.08	0.15
PBE-QIDH	0.40	0.54	0.10	0.12
PBE-QIDH-OS	1.30	1.70	0.15	0.36
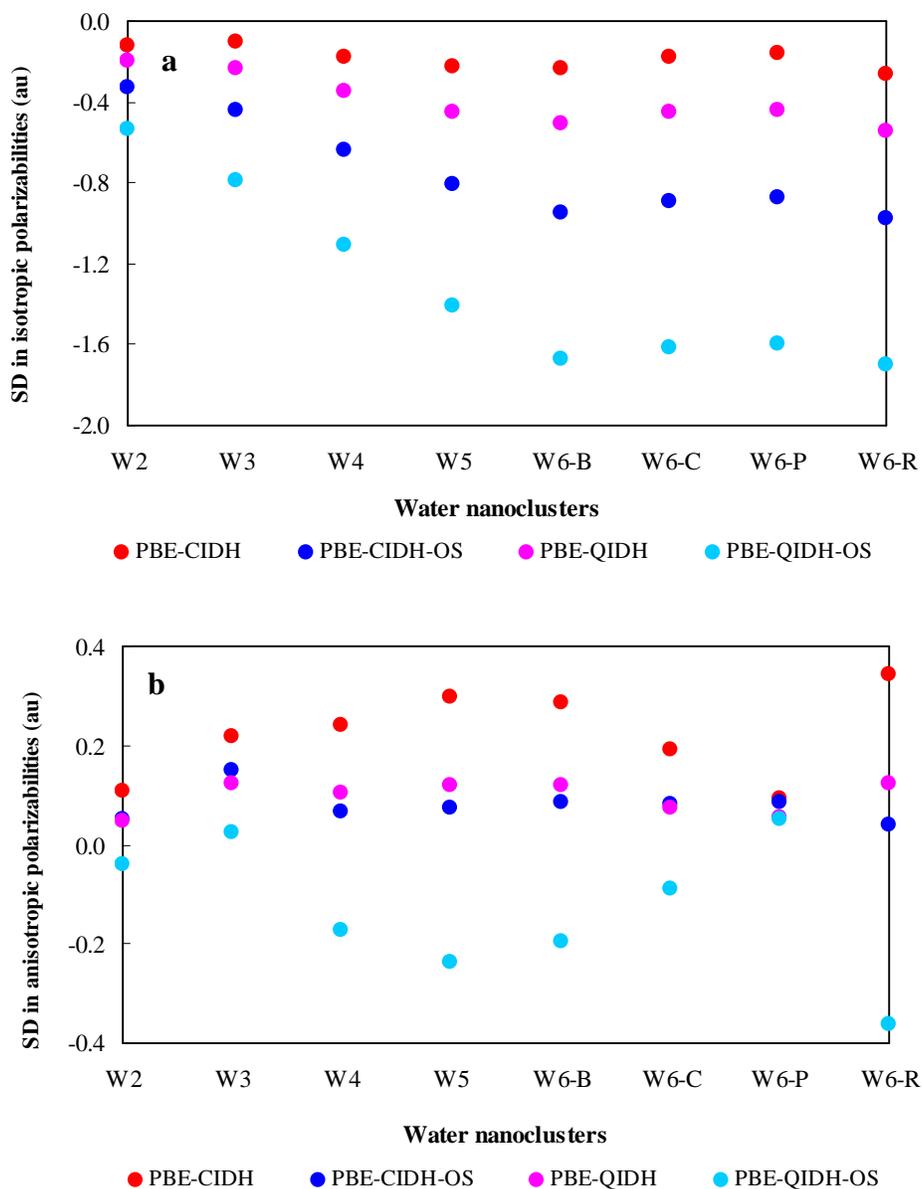
Fig. 2. Graphical representations of the signed deviations in the computed isotropic (a) and anisotropic (b) polarizabilities using the CIDHs and QIDHs.

accurate isotropic polarizability values are obtained by the PBE-CIDH functional with MAD = 0.18 a.u. and MaxAD = 0.27 a.u., lower than those provided from MP2 calculations (MAD = 1.03 a.u. and MaxAD = 1.32 a.u.) [23]. Since calculations of the AC-based DH density functionals are less expensive than MP2 calculations for large clusters, it is incentive that some of CI- and QI-based DHs outperform

MP2 for dipole polarizability calculations. The next functional is PBE-QIDH with MAD = 0.40 a.u. and MaxAD = 0.54 a.u., followed by PBE-CIDH-OS and PBE-QIDH-OS. On the other hand, it can also be concluded from Table 2 that the use of OS scheme in CIDHs and QIDHs does not improve the accuracy of the results of isotropic polarizabilities. Indeed, the same and opposite spin
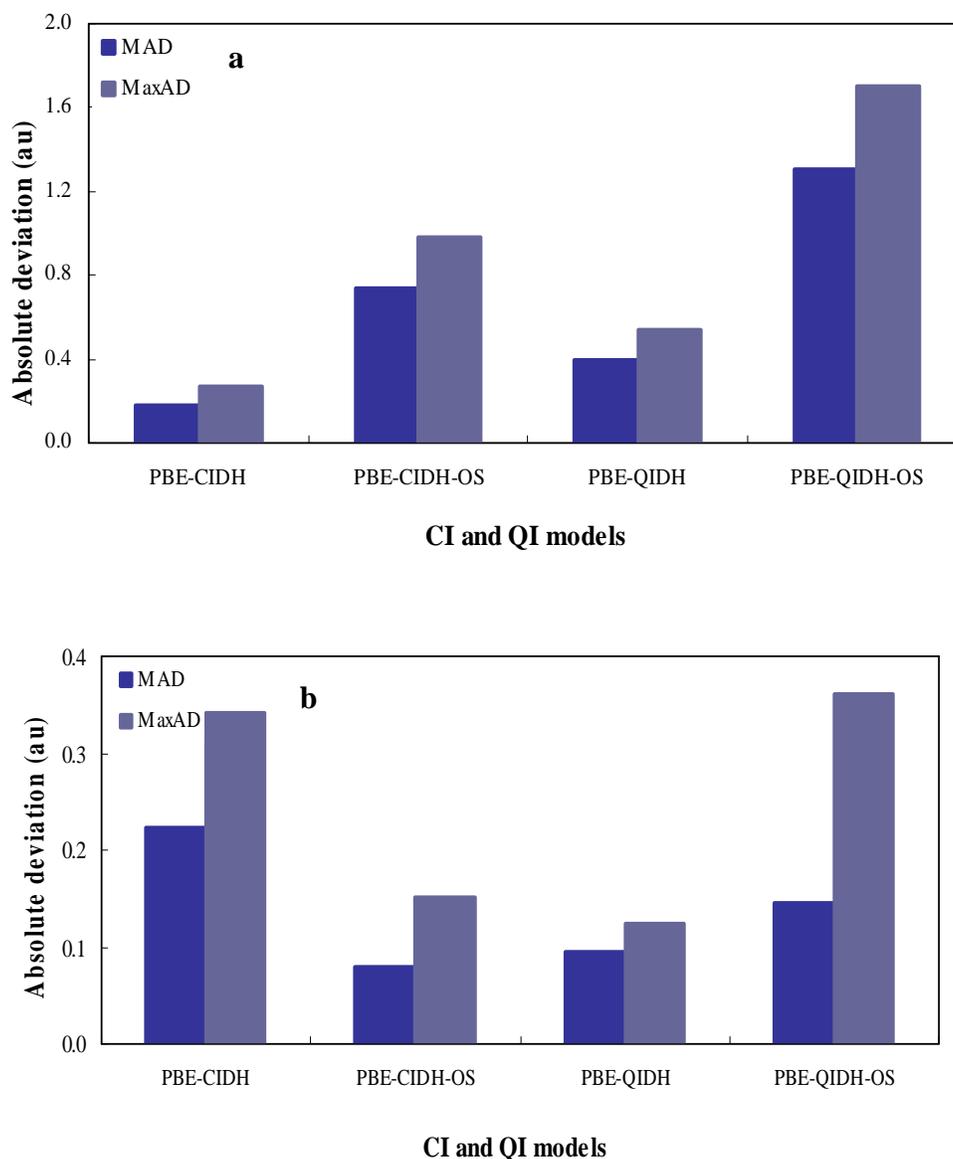
Fig. 3. Bar graphs of the MADs and MaxADs on the computed isotropic (a) and anisotropic (b) polarizabilities using the CIDHs and QIDHs models.

correlation components are respectively related to the long-range and short-range interactions and a model without each of them will not be able to predict reliable response properties. Concerning the results of anisotropic polarizabilities for water nanoclusters, we find however that the PBE-CIDH-OS (MAD = 0.08 a.u. and MaxAD = 0.15 au) and PBE-QIDH (MAD = 0.10 a.u. and MaxAD = 0.12

a.u.) give the lowest deviations, followed by the two functionals PBE-QIDH-OS and PBE-CIDH.

Although our emphasis in this work is to compare the DH functionals based on CI and QI functions for estimation of the dipole polarizabilities of water nanoclusters, it is also important to further assess the results of these modern models with respect to those obtained using other XC

functionals. The chosen functionals for this purpose are as follows: parameterized DH functionals B2-PLYP [1] and B2GP-PLYP (as a General Purpose functional) [6] and the two parameter-free DHs, PBE0-DH [13] and PBE0-2 [16]. The values of MADs for B2-PLYP, B2GP-PLYP, PBE0-DH and PBE0-2 are, respectively, 1.79, 0.96, 0.04 and 0.17 a.u. on the isotropic polarizabilities and 0.56, 0.28, 0.28 and 0.10 a.u. on the anisotropic polarizabilities. Comparing these results with those obtained using the best performing DH functionals in this work, PBE-CIDH and PBE-CIDH-OS, we find that the performance of PBE-CIDH functional is better than B2-PLYP and B2GP-PLYP functionals, though its accuracy does not reach the PBE0-DH in the case of isotropic polarizabilities. It is noted here that, the PBE0-DH model has been constructed based on LS1DH scheme, Eq. (2), and contains no fitted parameters but the ratio of the included terms were determined using theoretical arguments as 12.5% for MP2 correlation and 50% for exact exchange [13]. In addition, good performance of PBE0-DH model has also been advocated for other energetic properties, see for instance Refs. [13,17], highlighting more analyses of the energy expression of such models toward new discoveries in the field of DH-DFT. About anisotropic polarizabilities, PBE-CIDH-OS and PBE0-2 functionals with nearly equivalent performance are better than the others.

On the whole, it can be deduced that the DH density functionals based on cubic integrand function perform better than approximations containing quadratic integrand function for response properties of water nanoclusters. Lastly, what we would like to highlight the most here is that such statistical analyses are not entire story but hopefully may be considered as a starting point for proposing the new models. It seems that a bright future lies ahead.

FINAL COMMENTS

To summarize, within this study we have unveiled the accountability of a few modern double-hybrid models based on cubic and quadratic integrand functions and their counterparts with spin-opposite-scaled scheme for dipole polarizabilities of water nanoclusters. Several key findings emerge from this work which can be outlined as follows. Although the tested CIDHs and QIDHs underestimate the isotropic polarizabilities, in the case of anisotropic

polarizabilities there is also overestimation of data for a few nanoclusters. The PBE-CIDH functional is the best performing functional for isotropic polarizability. Additionally, our results showed that for anisotropy calculations of water nanoclusters the PBE-CIDH-OS model outperforms other functionals. Altogether, the recommended functionals for predicting the dipole polarizabilities are PBE-CIDH, PBE-CIDH-OS, PBE-QIDH, and PBE0-DH which improve over both Møller-Plesset perturbation calculations and other DHs. Finally, DH-DFT methodologies and particularly adiabatic connection-based models free of empirical parameterizations should receive more considerations for further development of DH functionals with reduced computational cost to investigate the dipole polarizabilities of large water clusters and other hydrogen-bonded systems.

ACKNOWLEDGMENTS

REFERENCES

[1]   Grimme, S., Semiempirical hybrid density functional with perturbative second-order correlation. *J. Chem. Phys.*, **2006**, *124*, 034108-1-034108-16, DOI: 10.1063/1.2148954.

[2]   Zhang, I. Y.; Xu, X., Doubly hybrid density functional for accurate description of thermo-chemistry, thermochemical kinetics and nonbonded interactions. *Int. Rev. Phys. Chem.*, **2011**, *30*, 115-160, DOI: 10.1080/0144235X.2010.542618.

[3]   Sancho-García, J. C.; Adamo, C., Double-hybrid density functionals: Merging wavefunction and density approaches to get the best of both worlds. *Phys. Chem. Chem. Phys.,* **2013**, *15*, 14581-14594, DOI: 10.1039/c3cp50907a.

[4]   Goerigk, L.; Grimme, S., Double-hybrid density functionals. *WIREs Comput. Mol. Sci.*, **2014**, *4*, 576-600, DOI: 10.1002/wcms.1193.

[5]   Zhao, Y.; Lynch, B. J.; Truhlar, D. G., Doubly hybrid meta DFT: New multi-coefficient correlation and density functional methods for thermochemistry and

thermochemical kkinetics. *J. Phys. Chem. A,* **2004**, *108*, 4786-4791, DOI: 10.1021/jp049253v.

[6] Karton, A.; Tarnopolsky, A.; Lamère, J. -F.; Schatz, G. C.; Martin, J. M. L., Highly accurate first-principles benchmark data sets for the parametrization and validation of density functional and other approximate methods. Derivation of a robust, generally applicable, double-hybrid functional for thermochemistry and thermochemical kinetics. *J. Phys. Chem. A,* **2008**, *112*, 12868-12886, DOI: 10.1021/jp801805p**.**

[7] Sancho-García, J. C.; Pérez-Jiménez, A. J., Assessment of double-hybrid energy functionals for π-conjugated systems. *J. Chem. Phys.*, **2009**, *131*, 084108-1-084108-11, DOI: 10.1063/1.3212881.

[8] Kozuch, S.; Gruzman, D.; Martin, J. M. L., DSD-BLYP: A general purpose double hybrid density functional including spin component scaling and dispersion correction. *J. Phys. Chem. C,* **2010,** *114*, 20801-20808, DOI: 10.1021/jp1070852.

[9] Zhang, Y.; Xu, X.; Jung, Y.; Goddard III, W. A., A fast doubly hybrid density functional method close to chemical accuracy using a local opposite spin ansatz. *Proc. Natl. Acad. Sci. U.S.A.,* **2011**, *108*, 19896-19900, DOI: 10.1073/pnas.1115123108.

[10] Goerigk, L.; Grimme, S., Efficient and accurate double-hybrid-meta-GGA density functionals-evaluation with the extended GMTKN30 database for general main group thermochemistry, kinetics, and noncovalent interactions. *J. Chem. Theory Comput.*, **2011**, *7*, 291-309, DOI: 10.1021/ct100466k.

[11] Sharkas, K.; Toulouse, J.; Savin, A., Double-hybrid density-functional theory made rigorous. *J. Chem. Phys.*, **2011**, *134*, 064113-1- 064113-9, DOI: 10.1063/1.3544215.

[12] Toulouse, J.; Sharkas, K.; Brémond, E.; Adamo, C., Rationale for a new class of double-hybrid approximations in density-functional theory. *J. Chem. Phys.*, **2011**, *135*, 101102-1-101102-3, DOI: 10.1063/1.3640019.

[13] Brémond, E.; Adamo, C., Seeking for parameter-free double-hybrid functionals: The PBE0-DH model. *J. Chem. Phys.*, **2011**, *135*, 024106-1-024106-6, DOI: 10.1063/1.3604569.

[14] Kozuch, S.; Martin, J. M. L., DSD-PBEP86: In search of the best double-hybrid DFT with spin-component scaled MP2 and dispersion corrections. *Phys. Chem. Chem. Phys.*, **2011**, *13*, 20104-20107, DOI: 10.1039/c1cp22592h.

[15] Zhang, I. Y.; Su, N. Q.; Brémond, E.; Adamo, C.; Xu, X., Doubly hybrid density functional xDH-PBE0 from a parameter-free global hybrid model PBE0. *J. Chem. Phys.*, **2012**, *136*, 174103-1-174103-8, DOI: 10.1063/1.3703893.

[16] Chai, J. -D.; Mao, S. -P., Seeking for reliable double-hybrid density functionals without fitting parameters: The PBE0-2 functional. *Chem. Phys. Lett.*, **2012**, *538*, 121-125, DOI: 10.1016/j.cplett.2012.04.045.

[17] Bousquet, D.; Brémond, E.; Sancho-García, J. C.; Ciofini, I.; Adamo, C., Is there still room for parameter free double hybrids? Performances of PBE0-DH and B2PLYP over extended benchmark Sets. *J. Chem. Theory Comput.*, **2013**, *9*, 3444-3452, DOI: 10.1021/ct400358f**.**

[18] Kozuch, S.; Martin, J. M. L., Spin-component-scaled double hybrids: An extensive search for the best fifth-rung functionals blending DFT and perturbation theory. *J. Comput. Chem.*, **2013**, *34*, 2327-2344, DOI: 10.1002/jcc.23391.

[19] Cornaton, Y.; Franck, O.; Teale, A. M.; Fromager, E., Analysis of double hybrid density-functionals along the adiabatic connection. *Mol. Phys.*, **2013**, *111*, 1275-1294, DOI: 10.1080/00268976.2013.783640.

[20] Su, N. Q.; Xu, X., Construction of a parameter-free doubly hybrid density functional from adiabatic connection. *J. Chem. Phys.*, **2014**, *140*, 18A512-1-18A512-15, DOI: 10.1063/1.4866457.

[21] Souvi, S. M. O.; Sharkas, K.; Toulouse, J., Double-hybrid density-functional theory with meta-generalized-gradient approximations. *J. Chem. Phys.*, **2014**, *140*, 084107-1-084107-6, DOI: 10.1063/1.4865963.

[22] Yu, F., Spin-component-scaled double-hybrid density functionals with nonlocal van der Waals correlations for noncovalent interactions. *J. Chem. Theory Comput.,* **2014**, *10*, 4400-4407, DOI: 10.1021/ct500642x.

[23] Alipour, M., A novel recipe for double-hybrid density

functional computations of linear and nonlinear polarizabilities of molecules and nanoclusters. *J. Phys. Chem. A,* **2014**, *118*, 5333-5342, DOI: 10.1021/ jp503959w.

[24] Brémond, E.; Sancho-García, J. C.; J. Pérez-Jiménez, A.; Adamo, C., Double-hybrid functionals from adiabatic-connection: The QIDH model. *J. Chem. Phys.*, **2014**, *141*, 031101-1-031101-4, DOI: 10.1063/1.4890314.

[25] Alipour, M., Designing a paradigm for parameter-free double-hybrid density functionals through the adiabatic connection Path. *Theor. Chem. Acc.*, **2015**, *134*, 87-1-87-8, DOI: 10.1007/s00214-015-1689-4.

[26] Wykes, M.; Pérez-Jiménez, A. J.; Adamo C.; Sancho-García, J. C., The diene isomerization energies dataset: A difficult test for double-hybrid density functionals? *J. Chem. Phys.*, **2015**, *142*, 224105-1-224105-7, DOI: 10.1063/ 1.4922058.

[27] Kim, J.; Jung, Y., Analytical double-hybrid density functional based on the polynomial series expansion of adiabatic connection: A quadratic approximation. *J. Chem. Theory Comput.*, **2015**, *11*, 45-54, DOI: 10.1021/ct500660k.

[28] Alipour, M., Relative energies of water nanoclusters $(H_2O)_{20}$: Comparison of empirical and nonempirical double-hybrids with generalized energy-based fragmentation approach. *New J. Chem.*, **2015**, *39*, 5534-5539, DOI: 10.1039/c5nj00817d.

[29] Brémond, E.; Savarese, M.; Pérez-Jiménez, A. J.; Sancho-García, J. C.; Adamo, C., Systematic improvement of density functionals through parameter-free hybridization schemes. *J. Phys. Chem. Lett.*, **2015**, *6*, 3540-3545, DOI: 10.1021/ acs.jpclett.5b01581.

[30] Alipour, M., Further evidences on the quality of meta-GGA linearly scaled one-parameter double-hybrids for frontier orbital energies. *Chem. Phys. Lett.*, **2015**, *623*, 14-16, DOI: 10.1016/ j.cplett.2015.01.032.

[31] Harris, J., Adiabatic-connection approach to kohn-sham theory. *Phys. Rev. A,* **1984**, *29*, 1648-1659,

DIO: 10.1103/PhysRevA.29.1648.

[32] Grimme, S., Improved second-order Møller-Plesset perturbation theory by separate scaling of parallel- and antiparallel-spin pair correlation energies. *J. Chem. Phys.*, **2003**, *118*, 9095-9102, DOI: 10.1063/ 1.1569242.

[33] Jung, Y.; Lochan, R. C.; Dutoi, A. D.; Head-Gordon, M., Scaled opposite-spin second order Møller-Plesset correlation energy: An economical electronic structure method. *J. Chem. Phys.*, **2004**, *121*, 9793-9802, DOI: 10.1063/1.1809602.

[34] Perdew, J. P.; Schmidt, K., Density functional theory and its application to materials. *AIP Conf. Proc.*, **2001**, *577*, 1-20, DOI: 10.1063/1.1390175.

[35] Perdew, J. P.; Burke, K.; Ernzerhof, M., Generalized gradient approximation made simple. *Phys. Rev. Lett.*, **1996**, *77*, 3865-3868, DOI: 10.1103/PhysRevLett. 77.3865.

[36] Hammond, J. R.; Govind, N.; Kowalski, K.; Autschbach, J.; Xantheas, S. S., Accurate dipole polarizabilities for water clusters $n = 2$-12 at the coupled-cluster level of theory and benchmarking of various density functionals. *J. Chem. Phys.*, **2009**, *131*, 214103-1-214103-9, DOI: 10.1063/1.3263604.

[37] Maroulis, G., Static hyperpolarizability of the water dimer and the interaction hyperpolarizability of two water molecules. *J. Chem. Phys.*, **2000**, *113*, 1813-1820, DOI: 10.1063/1.481985.

[38] Maroulis, G., Hyperpolarizability of H_2O revisited: accurate estimate of the basis set limit and the size of electron correlation effects. *Chem. Phys. Lett.*, **1998**, *289*, 403-411, DOI: 10.1016/S0009-2614(98)00439-4.

[39] Frisch, M. J.; Trucks, G. W.; Schlegel, H. B.; Scuseria, G. E.; Robb, M. A.; Cheeseman, J. R.; Scalmani, G.; Barone, V.; Mennucci, B.; Petersson, G. A.; *et al*. *Gaussian 09*, revision A.02; Gaussian, Inc.: Wallingford, CT, **2009**.

[40] Segarra-Martí, J.; Merchán, A.; Roca-Sanjuán, D., *Ab initio* determination of the ionization potentials of water clusters $(H_2O)_n$ ($n = 2$-6). *J. Chem. Phys.*, **2012**, *136*, 244306-1-244306-11, DOI: 10.1063/1.4730301.